8g. Nuclear Fission[1]

WALTER D. LOVELAND

Oregon State University

8g-1. The Probability of Fission. *Spontaneous Fission Half Lives.* Table 8g-1 lists the known half lives for decay by spontaneous fission from the ground states of various nuclei.

Fission Cross Sections. Tables 8g-2 and 8g-3 give the values of the fission cross section in barns for the thermal-neutron-induced and 14-MeV neutron-induced fission of various nuclei. Similarly, Figs. 8g-1 to 8g-3 show the energy variation of the fission cross section for proton-, alpha-particle-, and photon-induced fission, respectively. Moderate excitation-energy-induced fission may occur after the emission of 0, 1, 2, . . . neutrons; and thus the observed fission properties are a combination of the charac-

[1] Work supported in part by the U.S. Atomic Energy Commission.

teristics of fission of many different isotopes with different excitation energies. Figure 8g-4 shows the ratio of neutron width to fission width versus mass of the fissioning nucleus and is very useful in sorting out these situations involving "multiple-chance" fission.

8g-2 Fission Product Distributions. *Mass Distributions.* Table 8g-4 is the well-known "Katcoff table" of radiochemically measured fission yields for the thermal-

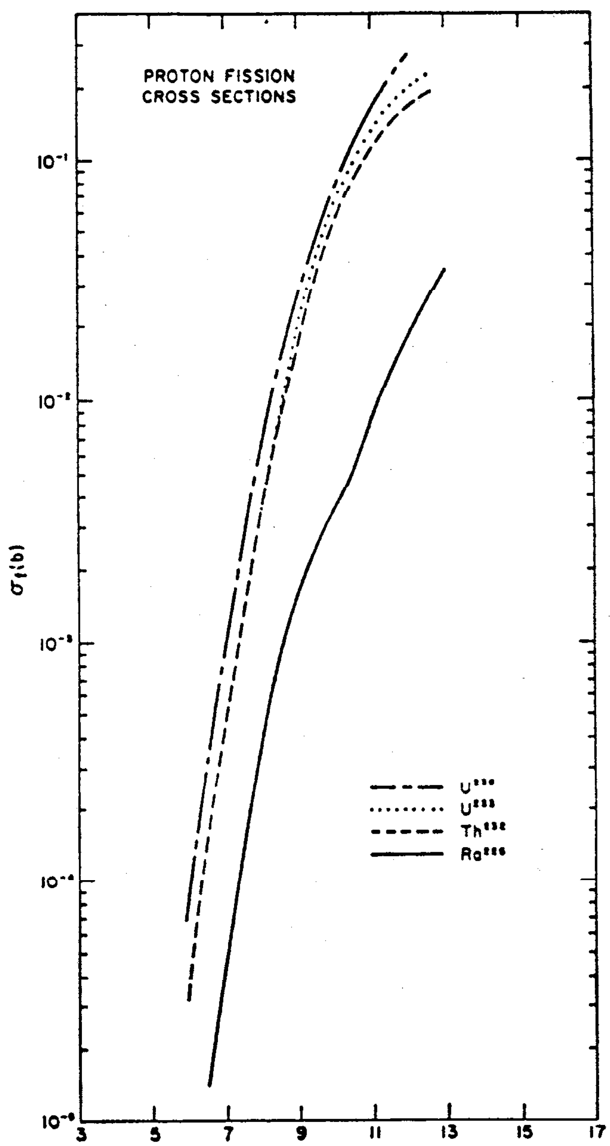

Fig. 8g-1. Energy variation of the fission cross section for proton-induced fission of various targets.

neutron-induced fission of U^{233}, U^{235}, and Pu^{239}. Figure 8g-5 summarizes the same information graphically. Figures 8g-6 and 8g-7 show similar mass-yield curves measured by physical techniques for a few representative cases of charged-particle-induced fission.

Charge Distributions. The most probably primary fragment charge *Zp* for fission fragments of mass *A* is shown in Fig. 8g-5 as a function of *A* for the thermal-neutron-

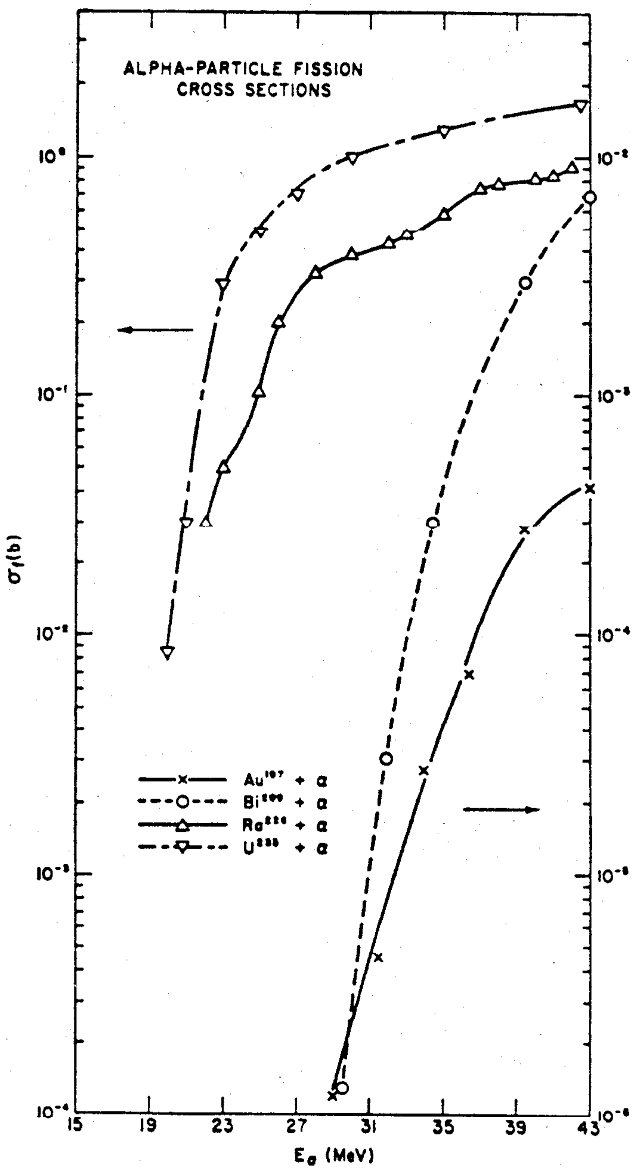

FIG. 8g-2. Energy variation of the fission cross section for α-particle-induced fission of various targets.

induced fission of U^{235}. The distribution of yields of fission products of charge Z is generally assumed to be gaussian for each fragment mass A and is given by

$$P(Z) = \frac{1}{\sqrt{c\pi}} \exp\left[-\frac{(Z - Zp)^2}{c}\right]$$

where c is an empirical constant. Wahl has found that a value of $c = 0.86$ fits a good deal of the data although there is no reason to expect c to have the same value for all mass numbers.

Kinetic Energy Release. Tables 8g-5 and 8g-6 show the average values of the fragment kinetic energies and masses prior to prompt neutron emission by the fragments for the thermal-neutron-induced fission of U^{235}, Pu^{239}, and Pu^{241} and the alpha-particle-

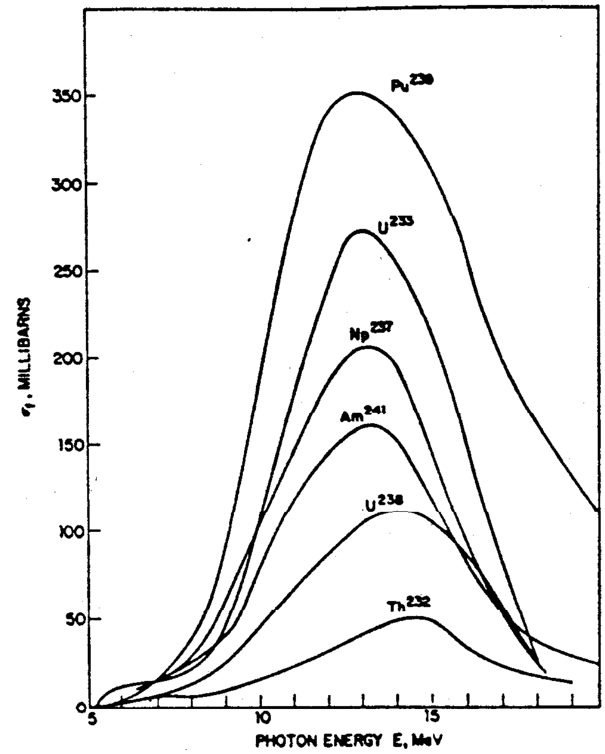

FIG. 8g-3. Energy variation of the fission cross section for photon-induced fission of various targets. [*L. Katz, A. P. Baerg, and F. Brown, Proc. 2d U. N. Conf. on Peaceful Uses of Atomic Energy* **15**, P, 200 (1958).]

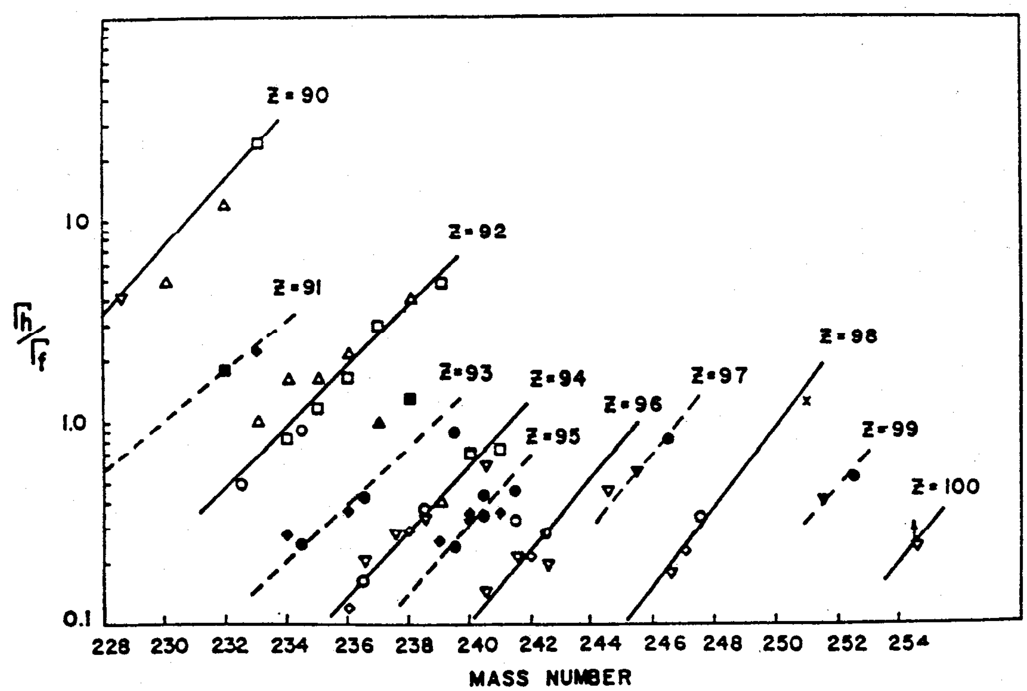

FIG. 8g-4. Neutron-width to fission-width ratios versus mass number of the fissioning nucleus. [*R. Vandenbosch and J. R. Huizenga, Proc. 2d U. N. Conf. on Peaceful Uses of Atomic Energy* **15**, 284 (1958).]

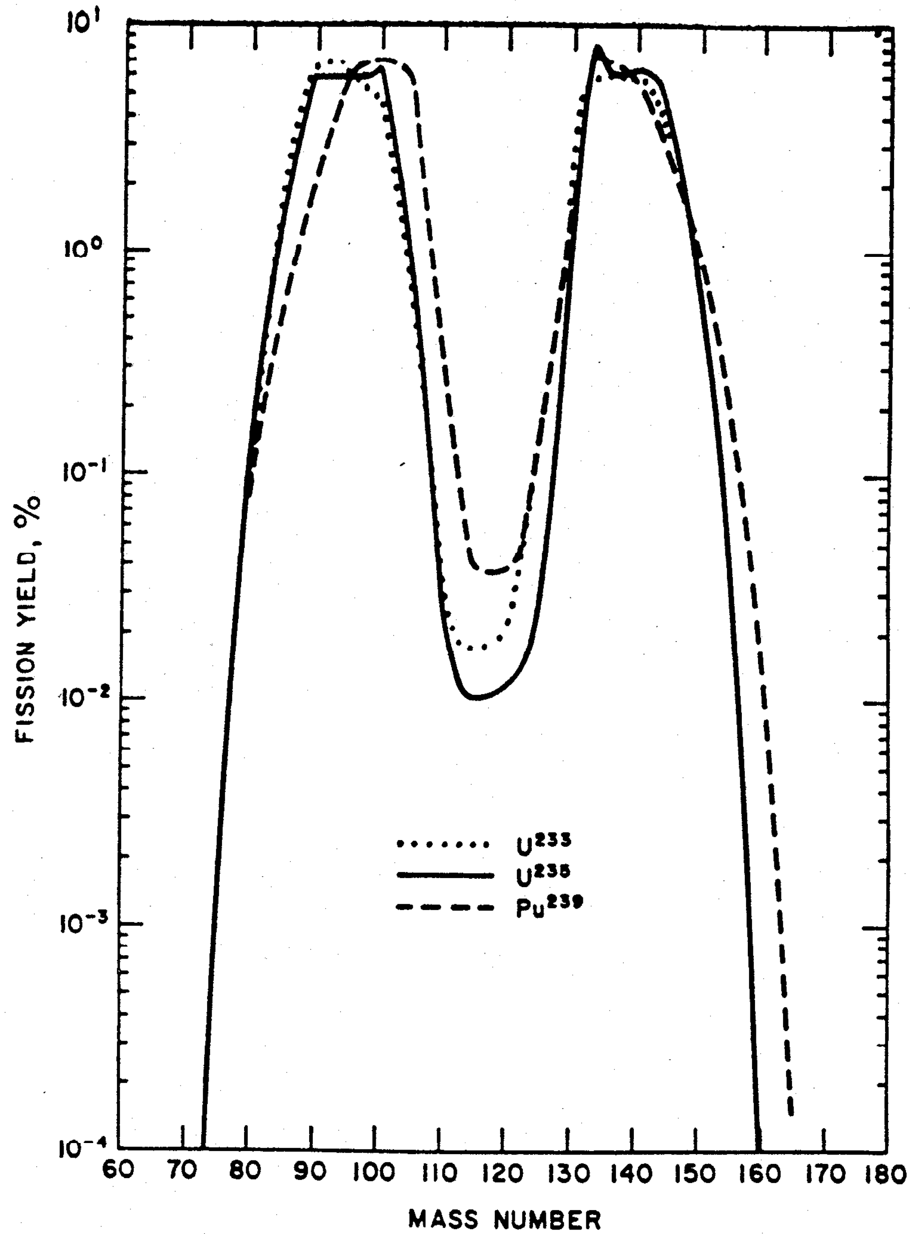

FIG. 8g-5. Fission-fragment mass distributions for the thermal-neutron-induced fission of U^{233}, U^{235}, and Pu^{239}.

induced fission of Th^{230}, Th^{232} and U^{233}, respectively. The variation in fragment kinetic energy with fragment mass is shown in Figs. 8g-9 to 8g-12 for these same fissioning nuclei.

Neutron Emission. Table 8g-7 shows the average number of prompt neutrons emitted per fission $\bar{\nu}$ for various nuclides. The distribution of neutron energies (as measured in the laboratory system) seems to be reasonably represented by a Maxwellian distribution of the form

$$N(E) = \left(\frac{2}{\pi^{\frac{1}{2}}T^{\frac{3}{2}}}\right) E^{\frac{1}{2}}e^{-E/T}$$

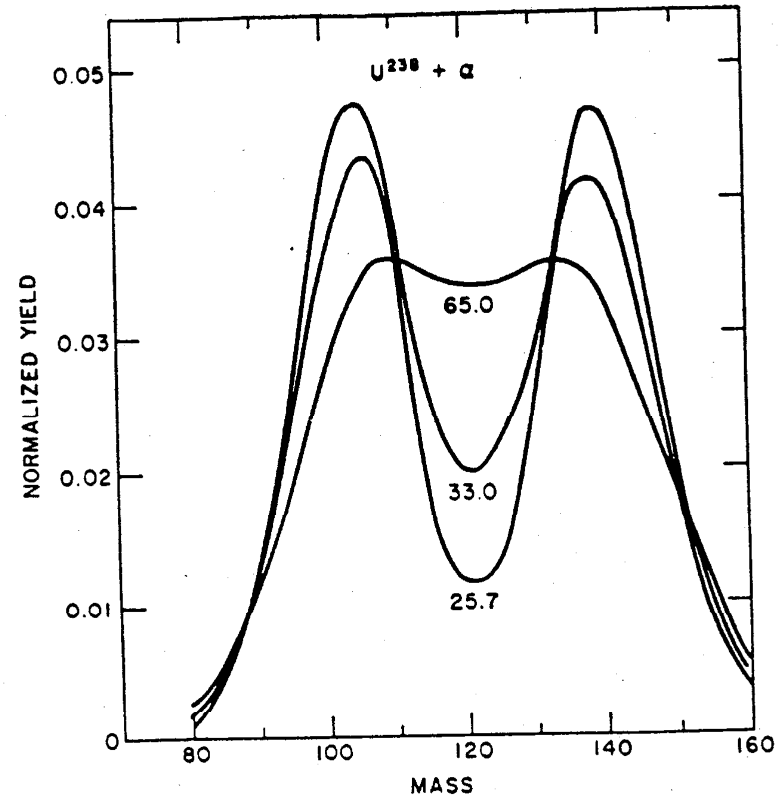

FIG. 8g-6. Mass-yield curves for the α-particle-induced fission of U^{238}. Yields are normalized to total of 200 percent. (*D. S. Burnett,* UCRL 11006.)

TABLE 8g-1. SPONTANEOUS FISSION HALF LIVES

Nuclide	Half Life	Nuclide	Half Life
Th^{230}	$\geq 1.5 \times 10^{17}$ y	Cm^{248}	$(4.6 \pm 0.5)(10^{6})$ y
Th^{232}	$>10^{21}$ y	Cm^{250}	$(1.13 \pm 0.05)(10^{4})$ y
U^{232}	$(8 \pm 5.5)(10^{13})$ y	Bk^{249}	$(1.87 \pm 0.09)(10^{9})$ y
U^{233}	$(1.2 \pm 0.3)(10^{17})$ y	Cf^{246}	(2.1 ± 0.3) y
U^{234}	1.6×10^{16} y	Cf^{248}	7×10^{3} y
U^{235}	$(3.5 \pm 0.9)(10^{17})$ y	Cf^{249}	$(6.87 \pm 0.33)(10^{10})$ y
U^{236}	2×10^{16} y	Cf^{250}	$(1.66 \pm 0.08)(10^{4})$ y
U^{238}	$(1.01 \pm 0.03)(10^{16})$ y	Cf^{252}	(8.55 ± 0.5) y
Np^{237}	$>10^{18}$ y	Cf^{254}	(60.5 ± 0.2) d
Pu^{236}	3.5×10^{9} y	Es^{253}	$(6.3 \pm 0.2)(10^{5})$
Pu^{238}	$(5 \pm 0.6)(10^{10})$ y	Es^{254}	$>2.5 \times 10^{7}$ y
Pu^{240}	$(1.340 \pm 0.015)(10^{11})$ y	Es^{255}	$2{,}440 \pm 140$ y
Fu^{242}	$(6.5 \pm 0.7)(10^{10})$ y	Fm^{252}	$>3{,}000$ d
Pu^{244}	$(2.5 \pm 0.8)(10^{10})$ y	Fm^{254}	228 ± 1 d
Am^{241}	$(2.3 \pm 0.8)(10^{14})$ y	Fm^{255}	$(1.0 \pm 0.6)(10^{4})$ y
Am^{243}	$(3.3 \pm 0.3)(10^{13})$	Fm^{256}	3 h
Cm^{240}	1.9×10^{6} y	Fm^{257}	~ 100 y
Cm^{242}	7.2×10^{6} y	No^{254}	~ 6 s
Cm^{244}	$(1.346 \pm 0.006)(10^{7})$ y	No^{256}	8.2 ± 1.0 s
Cm^{246}	$(1.78 \pm 0.04)(10^{7})$ y	Ku^{260}	(0.3 ± 0.1) s

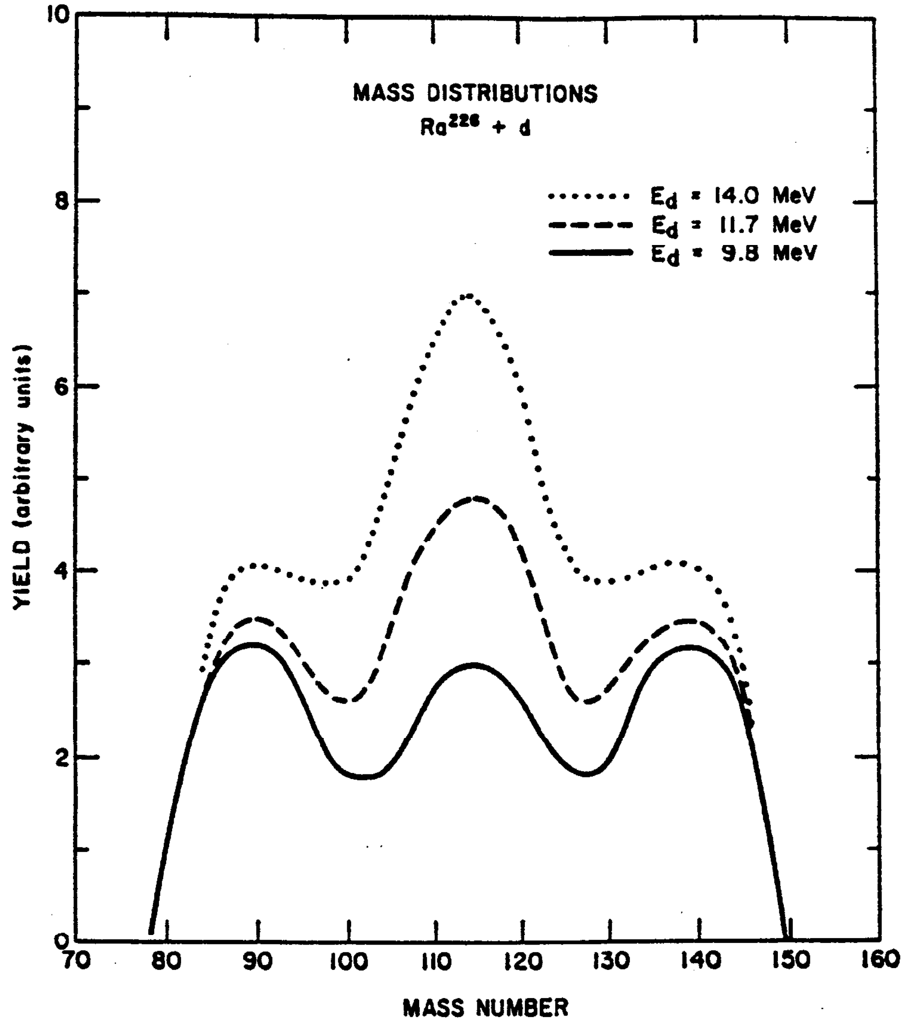

FIG. 8g-7. Mass distributions for the deuteron-induced fission of Ra^{226}. [*H. C. Britt, H. E. Wegner and J. Gursky, Phys. Rev.* **129**, 2239 (1963).]

TABLE 8g-2. THERMAL-NEUTRON-FISSION CROSS SECTIONS

Nuclide	$\sigma_f(b)$	Nuclide	$\sigma_f(b)$
Th^{229}	32 ± 3	Np^{234}	900 ± 300
Th^{230}	<0.001	Np_2^{236}(5000 y)	2800 ± 800
Th^{232}	(6 ± 2)(10^{-5})	Np^{237}	0.019 ± 0.003
Pa^{231}	0.010 ± 0.005	Pu^{238}	18.4 ± 0.9
U^{232}	72 ± 10	Pu^{239}	741 ± 4
U^{233}	524 ± 2	Pu^{240}	0.03 ± 0.045
U^{234}	<0.65	Pu^{241}	950 ± 30
U^{235}	577 ± 1	Am^{241}	3.13 ± 0.15
U^{238}	<0.5		

where T, the nuclear temperature, equals two-thirds the average energy, $\bar{E}$. Table 8g-8 gives some characteristics of fission neutron spectra while Table 8g-9 shows some *delayed* neutron yields from thermal-neutron-induced fission. The variation of the number of prompt neutrons emitted by a fragment of mass A with fragment mass is shown in Fig. 8g-13.

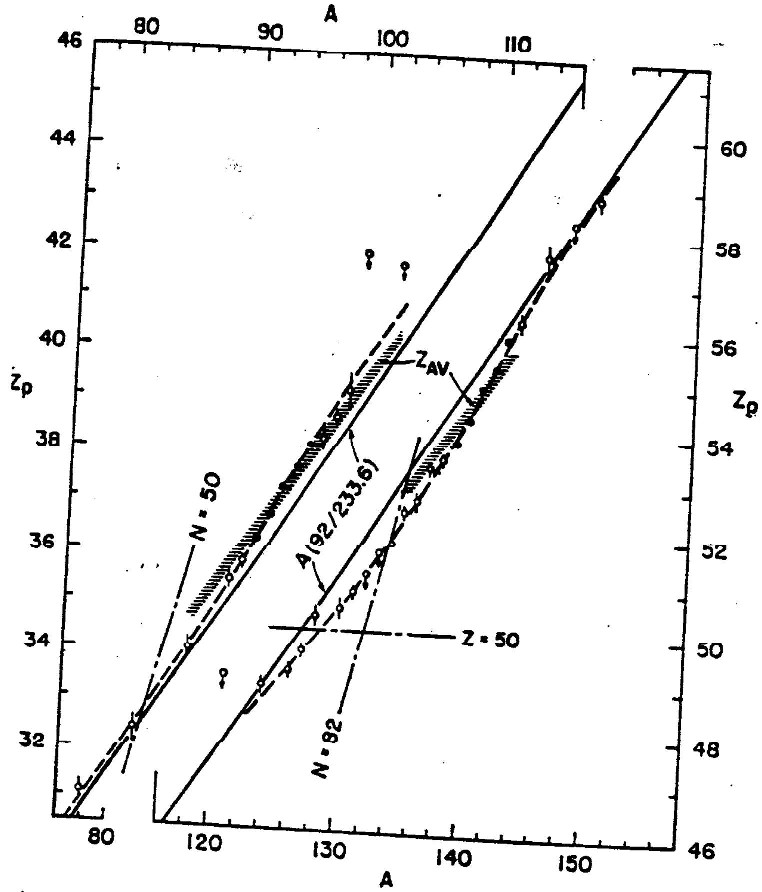

FIG. 8g-8. Empirical Zp values for fission products from U^{235} thermal-neutron fission. ●Zp values obtained from gaussian charge distribution curves determined by two or more fractional yields. ○Zp values estimated from the gaussian isobaric charge-distribution curve with $c = 0.86 \pm 0.15$ fitted to a single fractional yield value. Continuous lines represent the average charge density, $A(92/233.6)$. Broken lines represent an empirical Zp function derived from the points. [*A. C. Wahl, "Physics and Chemistry of Fission," vol.* I, 317 (1965).]

TABLE 8g-3. 14-MEV NEUTRON-FISSION CROSS SECTIONS

Nuclide	$\sigma_f(b)$
Bi^{209}	$(85 \pm 10)(10^{-9})$
Th^{230}	0.72 ± 0.15
Th^{232}	0.35 ± 0.03
U^{233}	2.25 ± 0.05
U^{235}	2.35 ± 0.100
U^{238}	1.23 ± 0.05
Np^{237}	2.5 ± 0.1
Pu^{239}	2.65 ± 0.10
Pu^{240}	2.4 ± 0.3
Pu^{241}	2.6 ± 0.1

Gamma-ray Emission and Beta Decay. The characteristics of the prompt gamma rays and beta particles emitted during the deexcitation of the fission products are given in Tables 8g-10 and 8g-11.

8g-3. Use of Semiconductor Radiation Detectors in Fission Studies. A great deal of the new and significant data in nuclear fission physics is due to the use of semi-

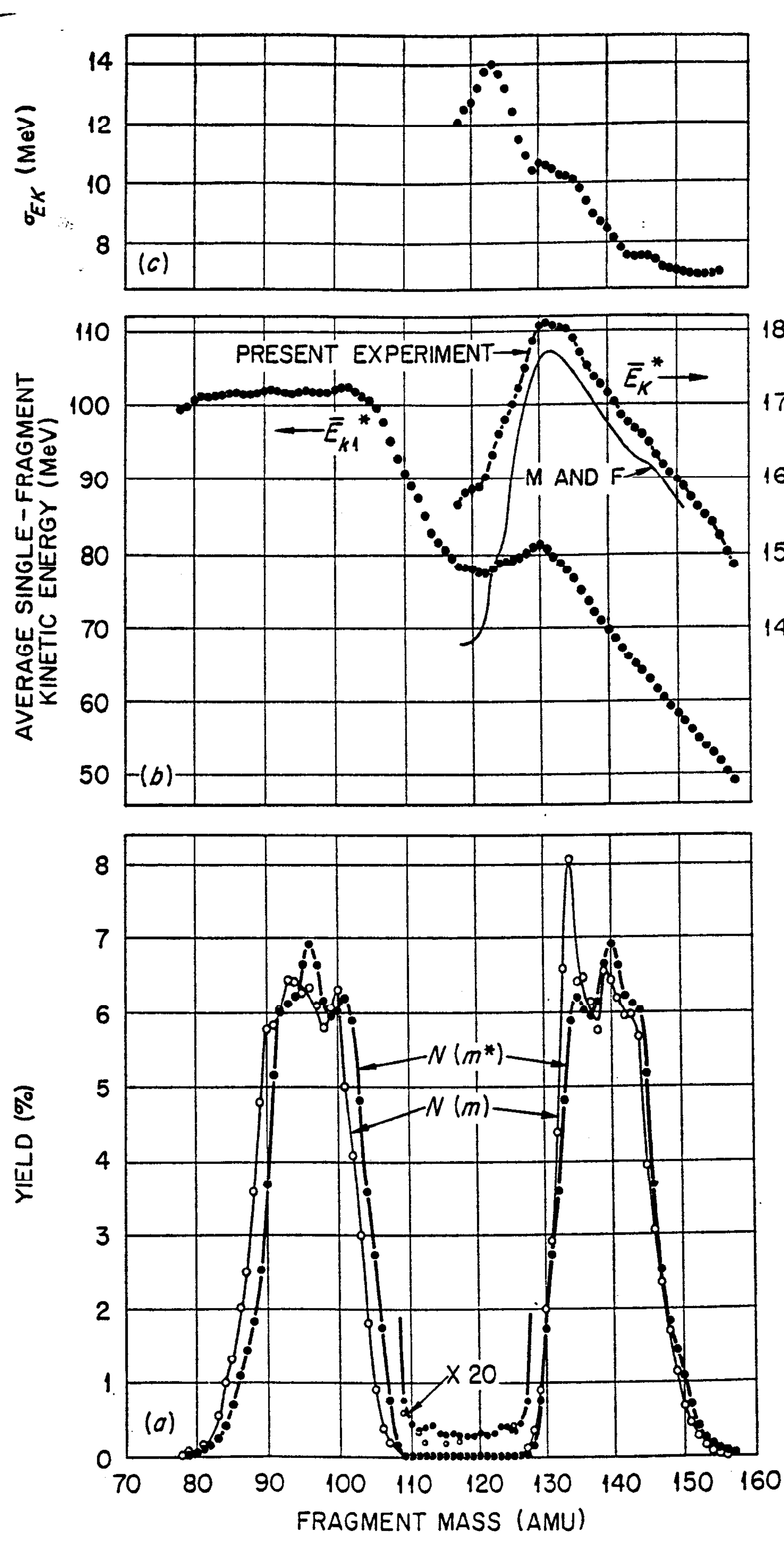

FIG. 8g-9. Study of fragment kinetic energy and mass for U^{239} thermal-neutron-induced fission. (*a*) Preneutron emission $N(m^*)$ and postneutron emission $N(m)$ mass distributions. (*b*) Average single-fragment and total preneutron emission kinetic energy as a function of mass. The total kinetic energy curve of Milton and Fraser is shown for comparison. (*c*) Root-mean-square width of total kinetic energy distribution as a function of fragment mass. [*H. W. Schmitt, J. H. Neiler, and F. J. Walter, Phys. Rev.* **141**, 1146

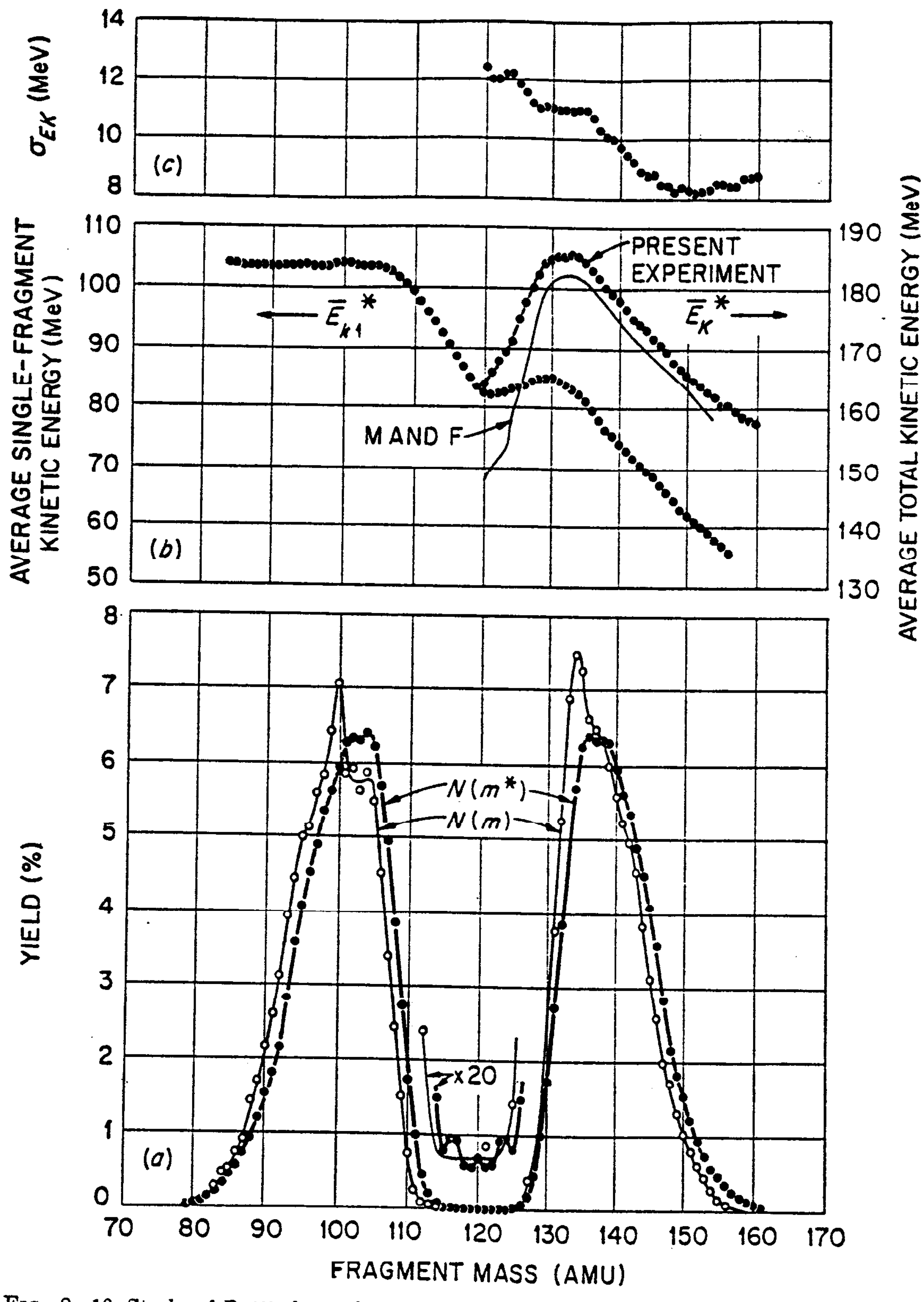

FIG. 8g-10. Study of Pu^{239} thermal-neutron fission. (*a*) Preneutron emission mass distribution corrected for resolution (closed circles); postneutron emission mass distribution points (open circles) are from Fickel and Tomkinson and in the symmetric region from Katcoff; the smooth curve at symmetry is from Walker. (*b*) Average single-fragment and total preneutron emission kinetic energy as a function of fragment mass; the curve of Milton and Fraser is shown for comparison. (*c*) Root-mean-square width of total kinetic energy distribution as a function of fragment mass. [*J. H. Neiler, F. J. Walter, and H. W. Schmitt, Phys. Rev.* **149**, 894 (1966).]

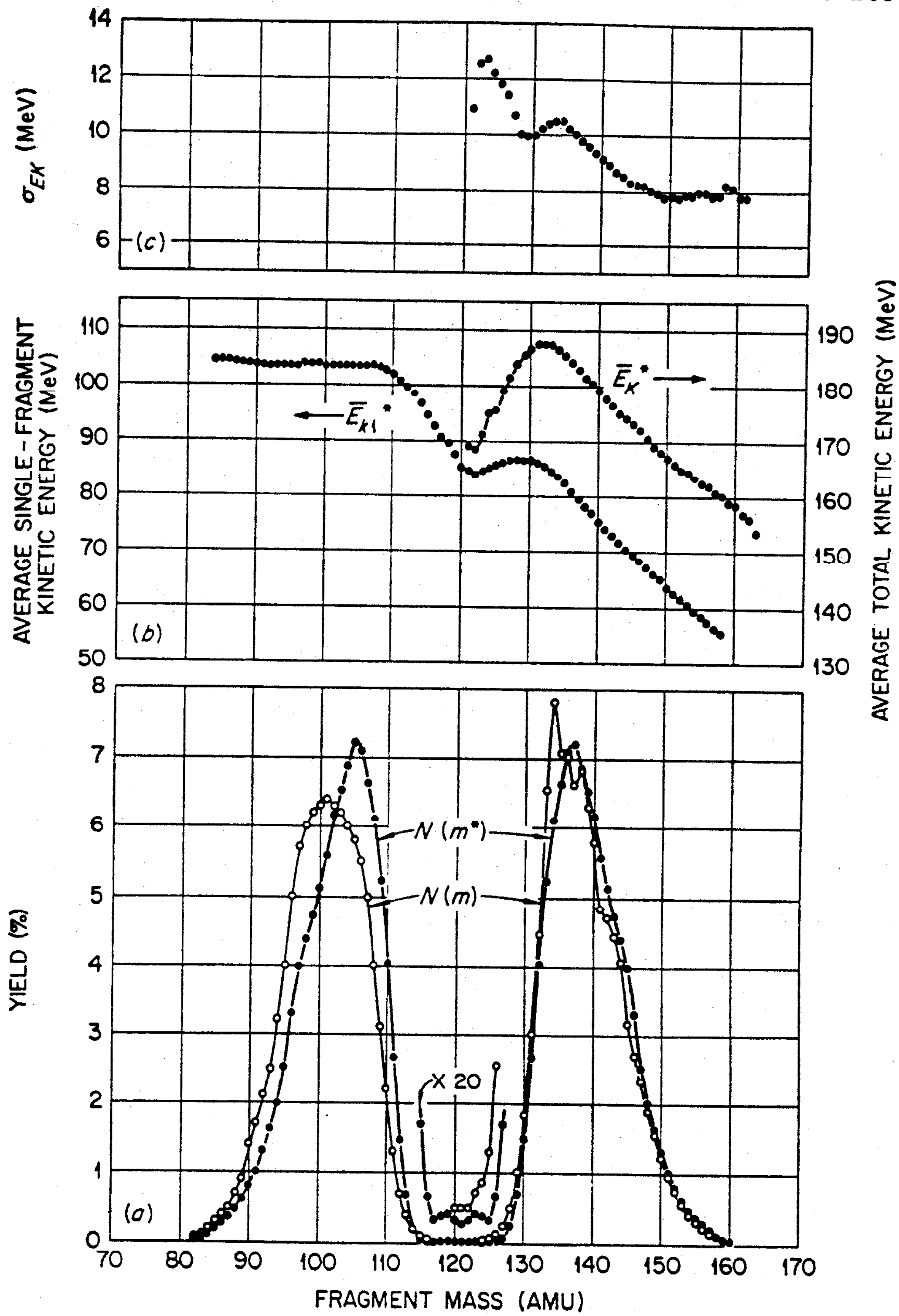

FIG. 8g-11. Study of Pu^{241} thermal-neutron fission. (*a*) Preneutron emission mass distribution corrected for resolution (closed circles); the postneutron emission mass yields shown (open circles) are from Farrar *et al.* (*b*) Average single fragment and total preneutron emission kinetic energy as a function of fragment mass. (*c*) Root-mean-square width of total kinetic energy distribution as a function of fragment mass. [*J. H. Neiler, F. J. Walter, and H. W. Schmitt, Phys. Rev.* **149,** 894 (1966).]

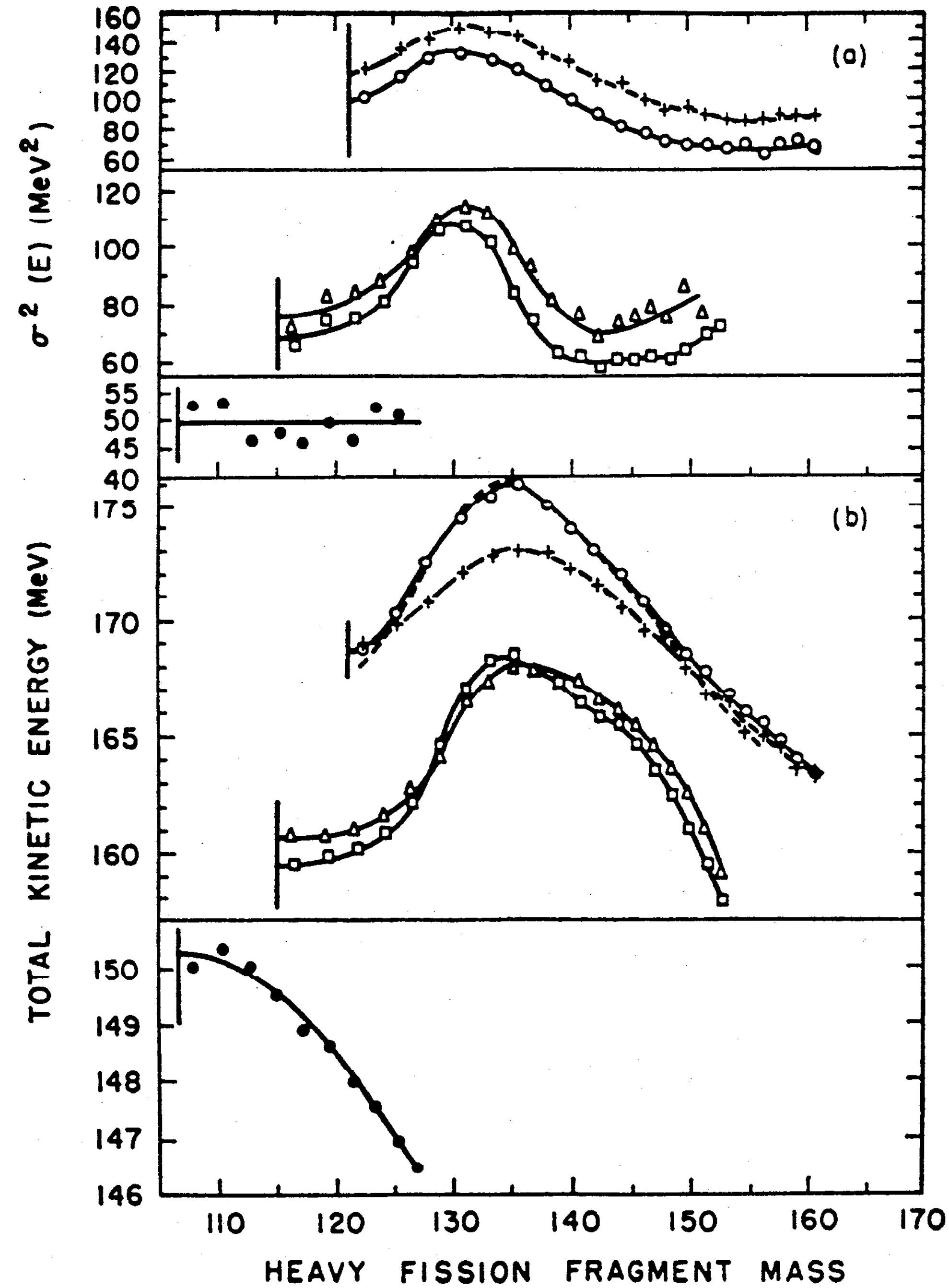

FIG. 8g-12. Initial total kinetic energy distributions as a function of the heavy fragment mass. (*a*) Variance of the total kinetic energy release. (*b*) Total kinetic energy release: ●Bi^{209} (42 MeV α,f); □Ra^{226} (30.8 MeV α,f); △Ra^{226} (38.7 MeV α,f); ○U^{238} (29.7 MeV α,f); + (42.0 MeV α,f). The dashed curve represents the data for U^{238} (29.7 MeV α,f) corrected for mass resolution. [*J. P. Unik and J. R. Huizenga, Phys. Rev.* **134,** B90 (1964).]

conductor radiation detectors rather than radiochemical techniques for the measurement of fission-fragment energies, masses, etc. Of particular importance in this regard has been the work of H. W. Schmitt and his coworkers[1] in formulating a mass-dependent energy calibration for these detectors (which corrects for the incomplete collection of the charge deposited by a heavy ion in the detector) and standards for the selection of good-quality detectors.

What one does to calibrate one's detectors in a given situation is to measure the fission-fragment pulse-height spectrum for a thin Cf^{252} or U^{235} source with the detectors. The fragment pulse-height spectrum is then used to define two points P_L and P_H, the midpoint of the light and heavy fragment peak, respectively, at three-fourths maximum. Then

$$E = (a + a'm)X + b + b'm$$

where E is the fragment kinetic energy, m is the mass, X is the pulse height, and a, a', b, b' are constants. The values of the constants are shown in Table 8g-12.

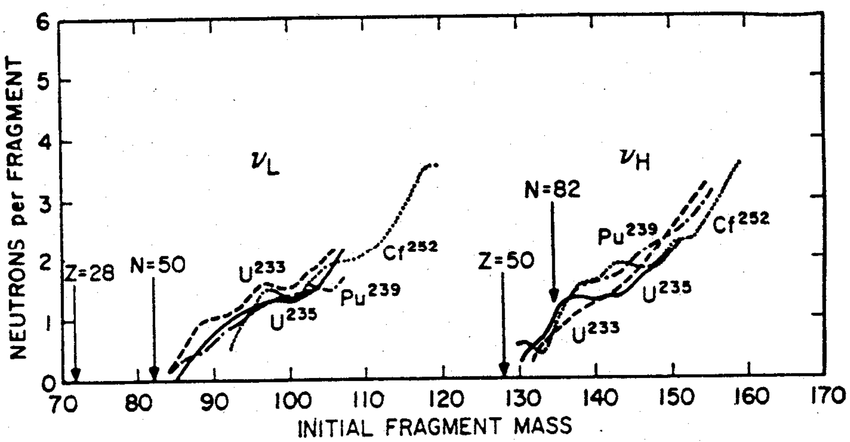

FIG. 8g-13. Neutron yields as a function of fragment mass derived from mass yield data. Also shown are the approximate initial fragment masses corresponding to various magic numbers based upon an unchanged charge-to-mass ratio (UCD) for the initial fragments. [*J. Terrell, Phys. Rev.* **127**, 880 (1962).]

Similarly, by measuring this pulse-height spectrum, one can define reasonable minimum characteristics for these heavy-ion detectors. Figure 8g-14 shows a typical Cf^{252} pulse-height spectrum with various shape parameters of the spectrum defined. Reasonable limits on these parameters are given in Table 8g-13. To get a feel for the importance of these parameters, note that a detector with $N_L/N_H = 1.25$ and $N_L/N_V = 2.73$ gave a factor of ~3 worse detector resolution than an acceptable detector.

8g-4. Cf^{252} Spontaneous Fission. Frequently, the measurement of fission-fragment energies, velocities, etc., is made relative to a primary standard, Cf^{252} spontaneous fission. This section presents the "best values" for the properties of Cf^{252} spontaneous fission as of June, 1968.

Fragment Kinetic Energies and Masses. Table 8g-14 summarizes the data of Whetstone concerning average fragment energies and masses. All quantities refer to preprompt neutron emission. Figure 8g-15 shows the variation in fragment kinetic energy with fragment mass.

Charge Distribution. The data on the most probable primary fragment charge Z_p as measured by K X-ray-fission coincidence measurements is given in Fig. 8g-16.

[1] *Phys. Rev.* **137**, B837 (1966); and *Nucl. Instr. Methods* **40**, 204 (1966).

TABLE 8g-4. THERMAL-NEUTRON-FISSION YIELDS (PERCENT) FROM U^{233}, U^{235}, AND Pu^{239}

Fission product	U^{233}	U^{235}	Pu^{239}	Fission product	U^{233}	U^{235}	Pu^{239}
47-hr Zn^{72}	....	1.6×10^{-5}	1.2×10^{-4}	10.3-hr Y^{93}	....	6.1	
4.9-hr Ga^{73}	....	1.1×10^{-4}		1.1×10^{6}-yr Zr^{93}	6.98	6.45	3.97
7.8-min Ga^{74}	....	3.5×10^{-4}		Stable Zr^{94}	6.68	6.40	4.48
11.3-hr Ge^{77}	0.011	0.0031		65-day Zr^{95}	6.1	6.2	5.8
38.7-hr As^{77}	0.021	0.0083		Stable Mo^{95}	6.11	6.27	5.03
2.1-hr Ge^{78}	....	0.020		Stable Zr^{96}	5.58	6.33	5.17
91-min As^{78}	....	0.020		23-hr Nb^{96}	6.5×10^{-3}	6.1×10^{-3}	3.6×10^{-3}
9.0-min As^{79}	....	0.056		17.0-hr Zr^{97}	....	5.9	5.5
Total Br^{80}	3.9×10^{-4}	1.0×10^{-6}		Stable Mo^{97}	5.37	6.09	5.65
57-min Se^{81m}	....	0.0084		52-min Nb^{98}	0.20	0.064	0.20
18.4-min Se^{81}	....	0.14		Stable Mo^{98}	5.15	5.78	5.89
35.9-hr Br^{82}	1.1×10^{-3}	4×10^{-5}		66.5-hr Mo^{99}	4.80	6.06	6.10
25-min Se^{83}	....	0.22		Stable Mo^{100}	4.41	6.30	7.10
2.4-hr Br^{83}	0.87	0.51	0.084	Stable Ru^{101}	2.91	5.0	5.91
Stable Kr^{83}	1.17	0.544	0.29	Stable Ru^{102}	2.22	4.1	5.99
6.0-min Br^{84}	....	0.019		39.7-day Ru^{103}	1.8	3.0	5.67
31.8-min Br^{84}	....	0.92		Stable Ru^{104}	0.94	1.8	5.93
Stable Kr^{84}	1.95	1.00	0.47	4.45-hr Ru^{105}	....	0.9	
39-sec Se^{85}	....	~1.1		36-hr Rh^{105}	....	....	3.9
10.6-yr Kr^{85}	0.58	0.293	0.127	1.01-yr Ru^{106}	0.24	0.38	4.57
Stable Rb^{85}	2.51	1.30	0.539	22-min Rh^{107}	....	0.19	
Stable Kr^{86}	3.27	2.02	0.76	13.4-hr Pd^{109}	0.044	0.030	1.40
18.6-day Rb^{86}	2.3×10^{-4}	2.9×10^{-5}	2.3×10^{-5}	7.6-day Ag^{111}	0.024	0.019	0.23
16-sec $Se^{(87)}$	....	~2		21.0-hr Pd^{112}	0.016	0.010	0.12
5×10^{10}-yr Rb^{87}	4.56	2.49	0.92	43-day Cd^{115m}	0.0011	0.0007	0.0031
Stable Sr^{88}	5.37	3.57	1.42	53-hr Cd^{115}	0.020	0.0097	0.0038
50.5-day Sr^{89}	5.86	4.79	1.71	Total 115	0.021	0.0104	0.041
28-yr Sr^{90}	6.43	5.77	2.25	3.0-hr Cd^{117m}	....	0.011	
9.7-hr Sr^{91}	5.57	5.81	2.43	27.5-hr Sn^{121}	0.018	0.015	0.043
58-day Y^{91}	5.1	~5.4	2.9	136-day Sn^{123}	....	0.0013	
Stable Zr^{91}	6.43	5.84	2.61	9.6-day Sn^{125}	0.052	0.013	0.071
2.7-hr Sr^{92}	....	5.3		2.0-yr Sb^{125}	....	0.021	
Stable Zr^{92}	6.64	6.03	3.14	91-hr Sb^{127}	0.60	0.13	0.39

TABLE 8g-4. THERMAL-NEUTRON-FISSION YIELDS (PERCENT) FROM U^{233}, U^{235}, AND Pu^{239} (*Continued*)

Fission product	U^{233}	U^{235}	Pu^{239}	Fission product	U^{233}	U^{235}	Pu^{239}
105-day Te^{127m}	....	0.035		33-day Ce^{141}	....	~6.0	5.1
57-min Sn^{128}	....	0.37		Stable Pr^{141}	6.4	....	(4.5)*
25.0-min I^{128}	....	3×10^{-5}		Stable Ce^{142}	6.83	6.01	5.01
37-day Te^{129m}	....	0.35		33-hr Ce^{143}	....	5.7	5.3
1.7×10^{7}-yr I^{129}	....	0.8		Stable Nd^{143}	5.99	6.03	4.57
2.6-min Sn^{130}	....	2.0		280-day Ce^{144}	4.5	~6.0	3.79
12.6 hr I^{130}	....	5×10^{-4}		5×10^{15}-yr Nd^{144}	4.61	5.62	3.93
30-hr Te^{131m}	....	0.44		Stable Nd^{145}	3.47	3.98	3.13
8.05-day I^{131}	2.9	~3.1	3.77	Stable Nd^{146}	2.63	3.07	2.60
Stable Xe^{131}	3.39	2.93	3.78	11.1-day Nd^{147}	....	~2.7	2.2
77-hr Te^{132}	4.4	~4.7	5.1	2.6-yr Pm^{147}	1.9	....	1.94
Stable Xe^{132}	4.64	4.38	5.26	1.3×10^{11}-yr Sm^{147}	1.98	2.36	2.07
20.8-hr I^{133}	....	~6.9	5.2	Stable Nd^{148}	1.34	1.71	1.73
5.27-day Xe^{133}	....	6.62	6.91	53.1-hr Pm^{149}	....	....	1.4
Stable Cs^{133}	5.78	6.59	6.91	Stable Sm^{149}	0.76	1.13	1.32
52.5-min I^{134}	....	7.8		Stable Nd^{150}	0.56	0.67	1.01
Stable Xe^{134}	5.95	8.06	7.47	80-yr Sm^{151}	0.335	0.44	0.80
6.7-hr I^{135}	5.5	6.1	5.7	Stable Sm^{152}	0.220	0.281	0.62
9.2-hr Xe^{135}	....	6.3		47-hr Sm^{153}	0.11	0.15	0.37
2.6×10^{6}-hr Cs^{135}	6.03	6.41	7.17	Stable Eu^{153}	0.13	0.169	
86-sec I^{136}	1.8	3.1	2.1	Stable Sm^{154}	0.045	0.077	0.29
Stable Xe^{136}	6.63	6.46	6.63	24-min Sm^{155}	....	0.033	0.23
13-day Cs^{136}	0.12	0.0068	0.11	4-yr Eu^{155}	....	0.033	
30-yr Cs^{137}	6.58	6.15	6.63	15.4-day Eu^{156}	0.011	0.014	0.11
Stable Ba^{138}	....	5.74	6.31	15.4-hr Eu^{157}	....	0.0078	
83-min Ba^{139}	6.45	6.55	5.87	60-min Eu^{158}	....	0.002	
12.8-day Ba^{140}	5.4	6.35	5.4	18.0-hr Gd^{159}	....	0.00107	0.021
Stable Ce^{140}	6.47	6.44	5.60	6.9-day Tb^{161}	....	7.6×10^{-5}	0.0039
3.8-hr La^{141}	7.1	6.4	5.7	82-hr Dy^{166}	....	....	6.8×10^{-5}

Reprinted from S. Katcoff, *Nucleonics* **18**(11), 203.

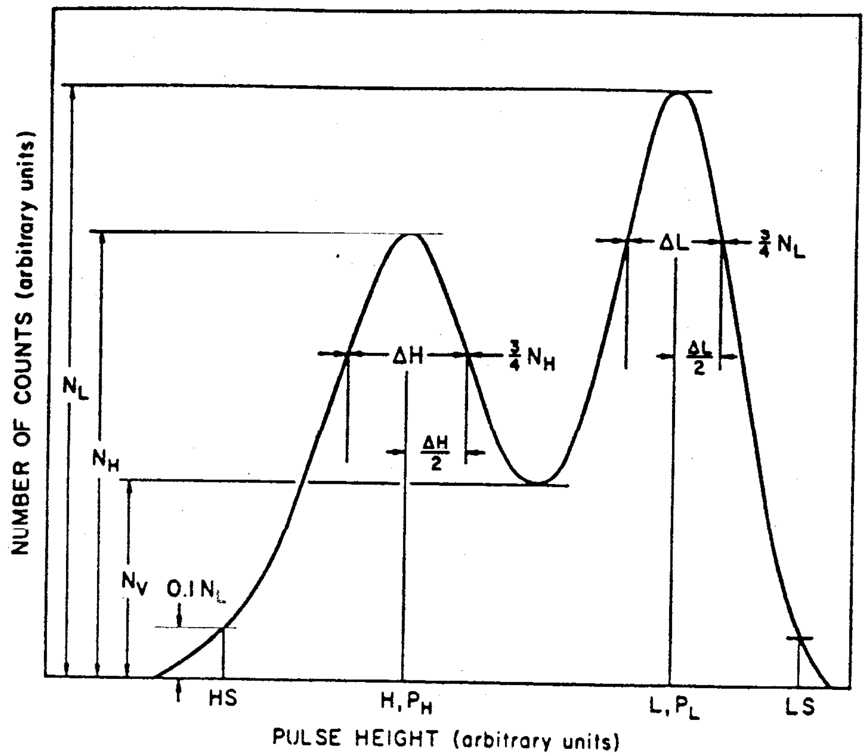

FIG. 8g-14. Shape parameters for Cf^{252} fission-fragment pulse-height distribution.

TABLE 8g-5. AVERAGE FRAGMENT ENERGIES AND MASSES FOR THERMAL-NEUTRON-INDUCED FISSION

Target nucleus	U^{235}	Pu^{239}	Pu^{241}
Total kinetic energy E_K	171.9 ± 1.4	177.7 ± 1.8	179.6 ± 1.8
σ_{E_K}	10.9	11.09	11.46
Kinetic energy, light fragment E_L	101.56	103.2 ± 1.0	103.2 ± 1.0
Kinetic energy, heavy fragment E_H	70.34	74.5 ± 0.8	76.3 ± 0.8
Mass, light fragment M_L	96.57	100.34	102.58
Mass, heavy fragment M_H	139.43	139.66	139.42
$\sigma_{M_L} = \sigma_{M_H}$	5.36	6.01	5.71

All quantities above are average quantities prior to prompt neutron emission by the fragments. Values are those of H. W. Schmitt, J. H. Neiler, and F. J. Walter, *Phys. Rev.* **141**, 1146 (1966); and J. H. Neiler, F. J. Walter, and H. W. Schmitt, *Phys. Rev.* **149**, 894 (1966).

Neutron Distribution. The average number of prompt neutrons emitted in the spontaneous fission of Cf^{252} is 3.771 ± 0.030. The properties of the neutron distribution in angle, energy, and number are shown in Figs. 8g-17 to 8g-20.

Gamma-ray Distribution. The gamma-ray yield as a function of fragment mass is shown in Fig. 8g-21. The average number of photons per fission is 10.3, and the average photon energy released per fission is 8.2 MeV.

Charged-particle Yields. The yield of charged particles emitted in Cf^{252} spontaneous fission is given in Table 8g-15.

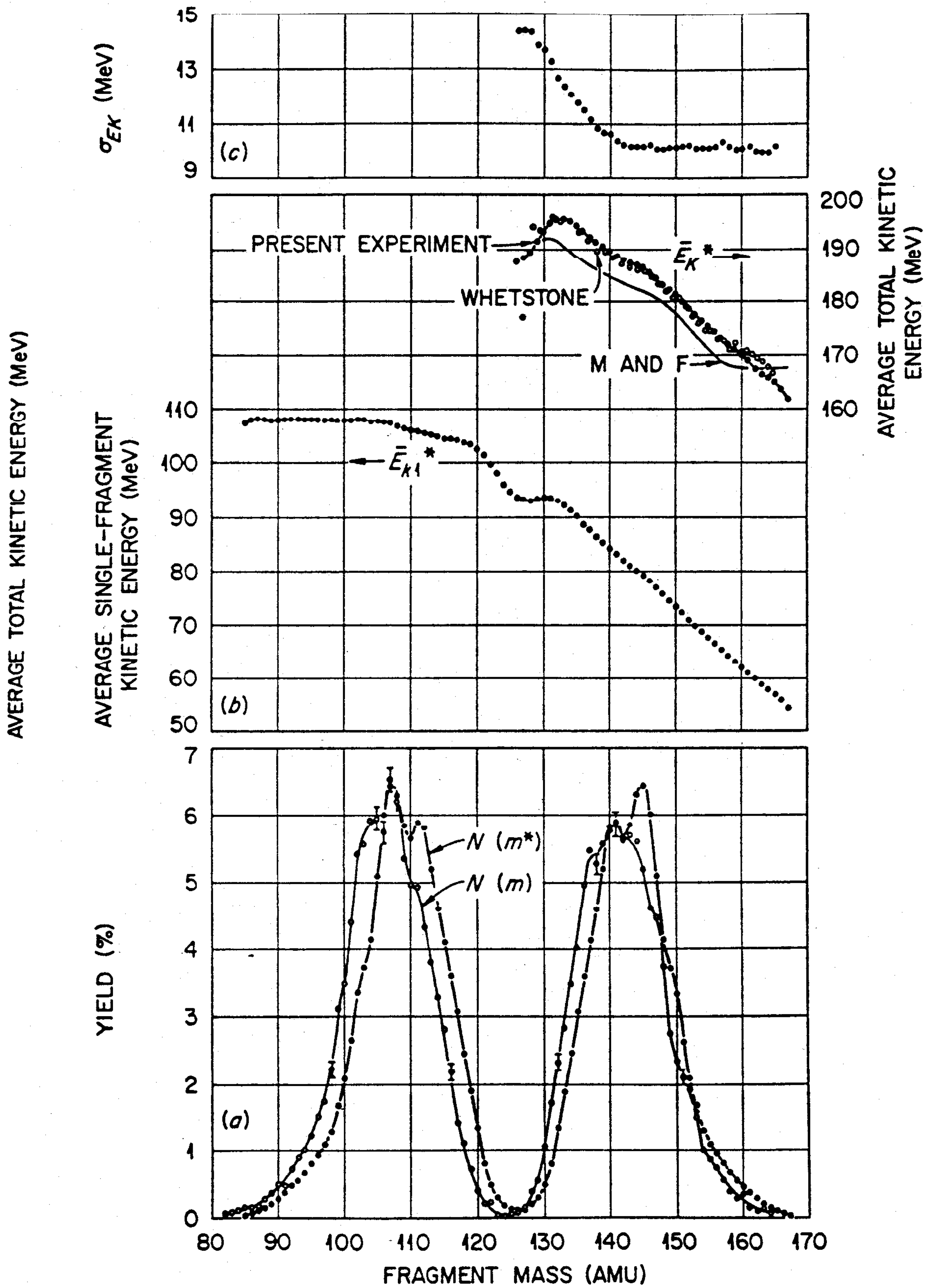

FIG. 8g-15. Study of Cf^{252} spontaneous fission. (*a*) Preneutron emission mass distribution $N(m^*)$ corrected for mass resolution; the postneutron-emission mass distribution $N(m)$ is from Schmitt (1965). (*b*) Average single-fragment and total preneutron emission kinetic energy as a function of mass; the total kinetic energy curves of Whetstone and Milton and Fraser are shown for comparison. (*c*) Root-mean-square width of total kinetic energy distribution as a function of fragment mass. [*H. W. Schmitt, J. H. Neiler, and F. J. Walter, Phys. Rev.* **141**, 1146 (1966).]

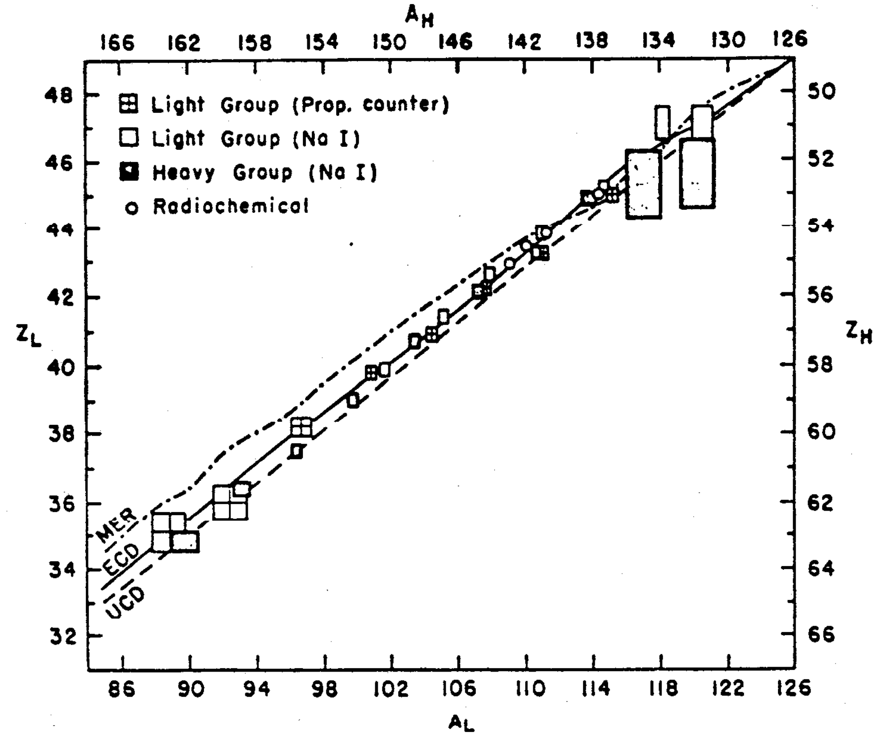

FIG. 8g-16. Average primary nuclear charge as a function of primary fragment mass in spontaneous fission of Cf^{252}. The size of the data symbol represents estimated errors in determinations of Z and A. The charge and mass of the light group (Z_L, A_L) and heavy group (Z_H, A_H) fragments are folded around symmetric fission ($Z = 49$, $A = 126$). Curves for various postulates of charge division are identified as MER (·—·), maximum energy release; ECD (——), equal charge displacement; and UCD (- - -), unchanged charge distribution. [*L. E. Glendenin and J. P. Unik, Phys. Rev.* **140**, B1301 (1965).]

TABLE 8g-6. AVERAGE FRAGMENT ENERGIES AND MASSES FOR CHARGED-PARTICLE-INDUCED FISSION

Target and reaction	E_α	E_K	E_L	E_H	M_L	M_H	σ_M
$Th^{230} + \alpha$..................	25.7	167.5	97.0	70.5	98.4	135.6	8.7
	29.7	166.0	95.6	70.4	99.2	134.8	9.1
$Th^{232} + \alpha$..................	21.8	169.1	99.5	69.6	97.0	139.0	7.9
	25.7	168.2	98.1	70.1	98.3	137.7	8.2
	29.5	167.0	96.9	70.2	99.1	136.9	8.8
$U^{233} + \alpha$..................	21.8	176.3	101.7	74.6	100.2	136.8	8.4
	25.7	174.9	99.8	75.1	101.7	135.3	8.8
	29.7	174.2	98.9	75.4	102.4	134.6	9.0

TABLE 8g-7. AVERAGE NUMBER OF PROMPT NEUTRONS EMITTED PER FISSION FOR VARIOUS NUCLIDES

Fissioning nucleus	Bondarenko (1958)[a]	Leachman (1958)[a]	Recent values
	Spontaneous Fission		
U^{238}	2.30 ± 0.20	....	1.97 ± 0.07[b]
Pu^{236}	2.17 ± 0.20		
Pu^{238}	2.28 ± 0.10		
Pu^{240}	2.23 ± 0.05	2.26 ± 0.05 2.22 ± 0.11	2.154 ± 0.028[b] 2.189 ± 0.026[c]
Pu^{242}	2.28 ± 0.13	2.18 ± 0.09	
Cm^{242}	2.59 ± 0.11		
Cm^{244}	2.82 ± 0.09		
Bk^{249}	3.72 ± 0.16		
Cf^{246}	2.92 ± 0.19		
Cf^{252}	3.84 ± 0.12	....	3.771 ± 0.031[c] 3.799 ± 0.034[d] 3.704 ± 0.015[e]
Cf^{254}	3.90 ± 0.14		
Fm^{254}	4.05 ± 0.19		
	Thermal Neutron Fission		
Th^{230}	2.13 ± 0.03		
U^{234}	2.52 ± 0.03	2.54 ± 0.04 2.55 ± 0.05	2.473 ± 0.026[c]
U^{236}	2.47 ± 0.03	2.47 ± 0.05 2.46 ± 0.03	2.425 ± 0.020[c] 2.369 ± 0.015[e] 2.417 ± 0.015[f]
Pu^{240}	....	2.88 ± 0.04 2.95 ± 0.06	2.831 ± 0.028[c]
Pu^{242}	....	3.03 ± 0.06	3.14 ± 0.06[g] 2.96 ± 0.08[h]
Am^{242}	3.14 ± 0.04		

* From J. Gindler and J. R. Huizenga, Nuclear Fission, in "Nuclear Chemistry," vol. II, L. Yaffe, ed., Academic Press, Inc., New York, 1968.
[a] I. I. Bondarenko, B. D. Kuzminov, L. S. Kutsayeva, L. I. Prokhorova, and G. N. Smirenkin, *Proc. U.N. Intern. Conf. Peaceful Uses At. Energy (Geneva)* **15**, 353 (1958). R. B. Leachman, *ibid.*, 229.
[b] Asplund-Nilsson, H. Condé, and N. Starfelt, *Nucl. Sci. Eng.* **15**, 213 (1963).
[c] J. C. Hopkins and B. C. Diven, *Nucl. Phys.* **48**, 433 (1963).
[d] I. Asplund-Nilsson, H. Condé, and N. Starfelt, *Nucl. Sci. Eng.* **16**, 124 (1963).
[e] D. W. Colvin and M. G. Sowerby, "Physics and Chemistry of Fission," vol. II, p. 25, IAEA, Vienna, 1965.
[f] H. Condé and M. Holmberg, *ibid*, p. 57.
[g] G. de Saussure and E. G. Silver, *Nucl. Sci. Eng.* **5**, 49 (1959).
[h] A. H. Jaffey, C. T. Hibdon, and R. Sjoblom, *J. Nucl. Energy*, pt. A, **11**, 21 (1959).

TABLE 8g-8. CHARACTERISTICS OF FISSION NEUTRON SPECTRA*

Fissile nuclide	Average energy $\bar{E}$, MeV	Maxwellian temperature, $T = 2\bar{E}/3$, MeV
$U^{233} + n_{th}$	1.98 ± 0.05†	1.32 ± 0.03
$U^{235} + n_{th}$	1.95 ± 0.05†	1.30 ± 0.03
$Pu^{239} + n_{th}$	2.03 ± 0.05†	1.35 ± 0.03
$Pu^{241} + n_{th}$	2.002 ± 0.051‡	1.335 ± 0.034
Cf^{252}	2.15 ± 0.08†	1.43 ± 0.05

* From J. Gindler and J. R. Huizenga, Nuclear Fission, in "Nuclear Chemistry," vol. II, L. Yaffe, ed., Academic Press, Inc., New York, 1968.
† J. Terrell, *Phys. Rev.* **127**, 880 (1967).
‡ A. B. Smith, R. Sjoblom, and J. H. Roberts, Phys. Rev. **123**, 2140 (1961).

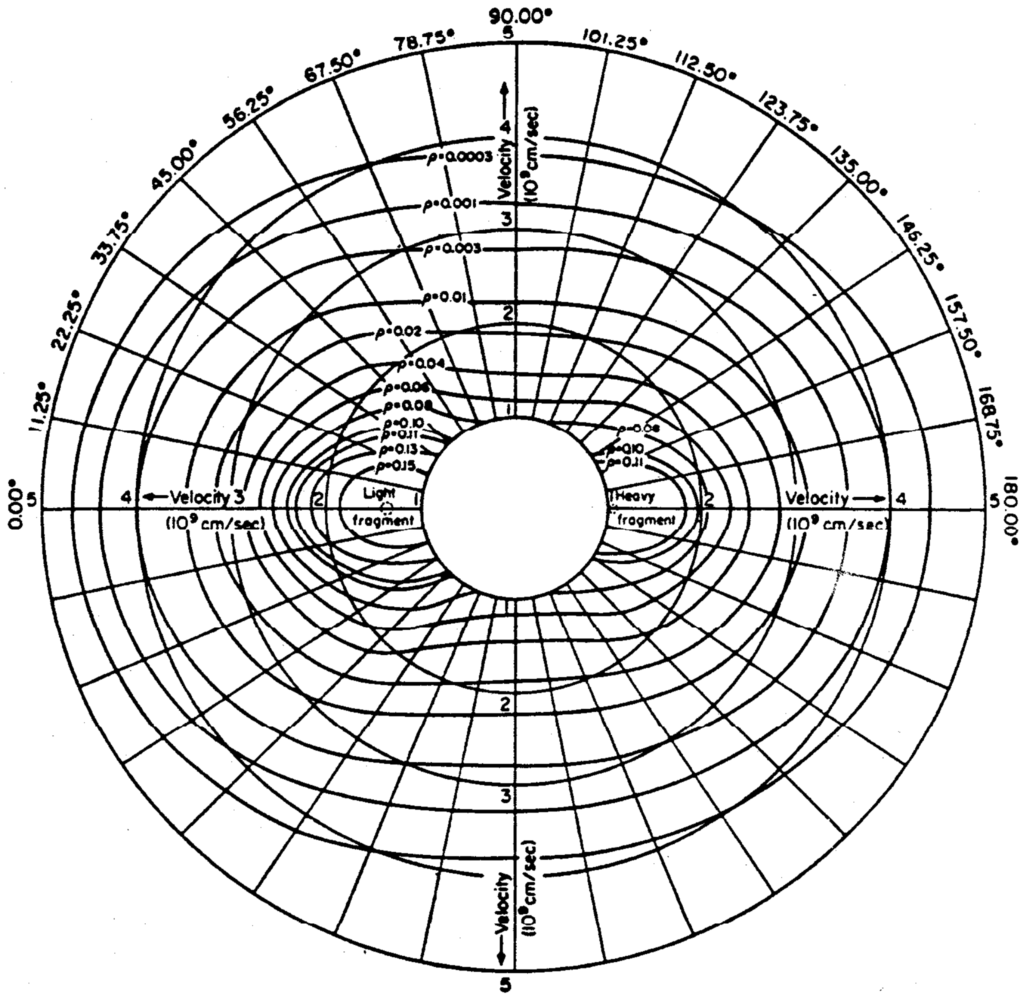

FIG. 8g-17. Contour diagram in polar coordinates of observed neutron density distribution $p(V,\phi)$ as a function of neutron velocity and angle. The contour lines are lines of constant neutron density. The average velocities of the light and heavy fragments are also shown. [*H. R. Bowman, S. G. Thompson, J. C. D. Milton, and W. J. Swiatecki, Phys. Rev.* **126,** 2120 (1962); **129,** 2133 (1963).]

TABLE 8g-9. ABSOLUTE YIELDS OF DELAYED NEUTRONS FROM THERMAL-NEUTRON-INDUCED FISSION*

Target fissile nuclide	*Delayed neutrons per fission*
U^{233}	0.0066 ± 0.0003†
U^{235}	0.0158 ± 0.0005†
Pu^{239}	0.0061 ± 0.0003†
Pu^{241}	0.0154 ± 0.0015‡

* From J. Gindler and J. R. Huizenga, Nuclear Fission, in "Nuclear Chemistry," vol. II, L. Yaffe' ed., Academic Press, Inc., New York, 1968.

† G. R. Keepin, T. F. Wimett, and R. K. Zeigler, *Phys. Rev.* **107,** 1044 (1957).

‡ S. A. Cox, *Phys. Rev.* **123,** 1735 (1961).

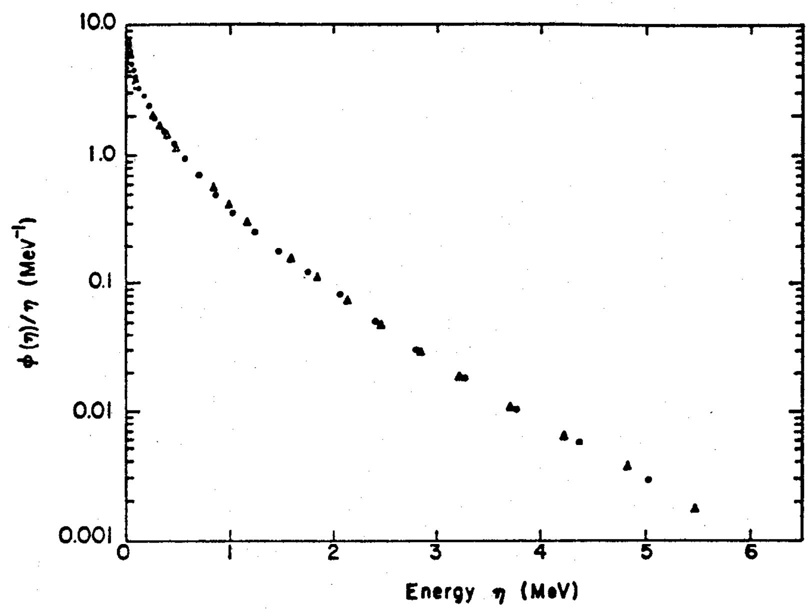

FIG. 8g-18. The center-of-mass neutron spectrum $\phi(\eta)$ divided by η, the neutron energy in the center-of-mass system. The dots represent neutrons emitted in the direction of the light fragments; the triangles represent neutrons emitted in the direction of the heavy fragments. The curve for the light fragments was reduced by the factor 1.16, the ratio of the number of neutrons from light fragments to the number from heavy fragments if all neutrons are emitted from moving fragments. See Fig. 8g-17 for reference.

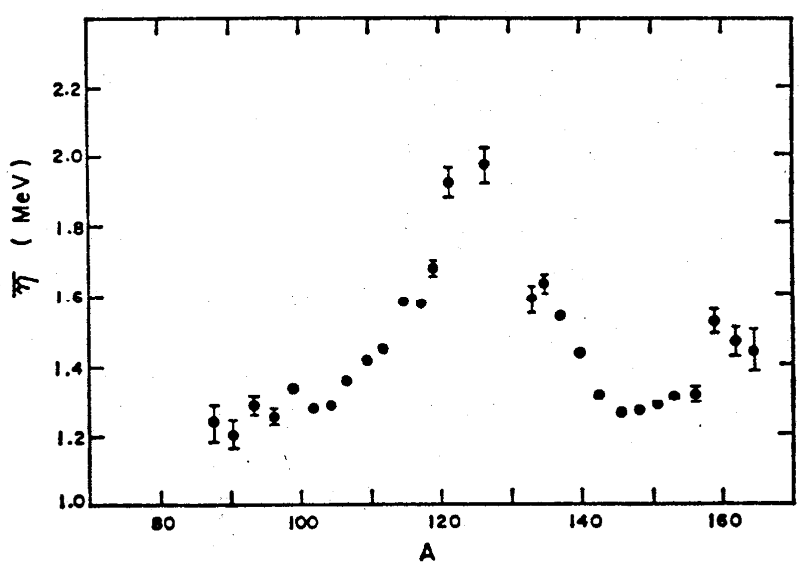

FIG. 8g-19. The average center-of-mass neutron kinetic energy as a function of fragment mass, corrected for mass resolution. For reference, see Fig. 8g-17.

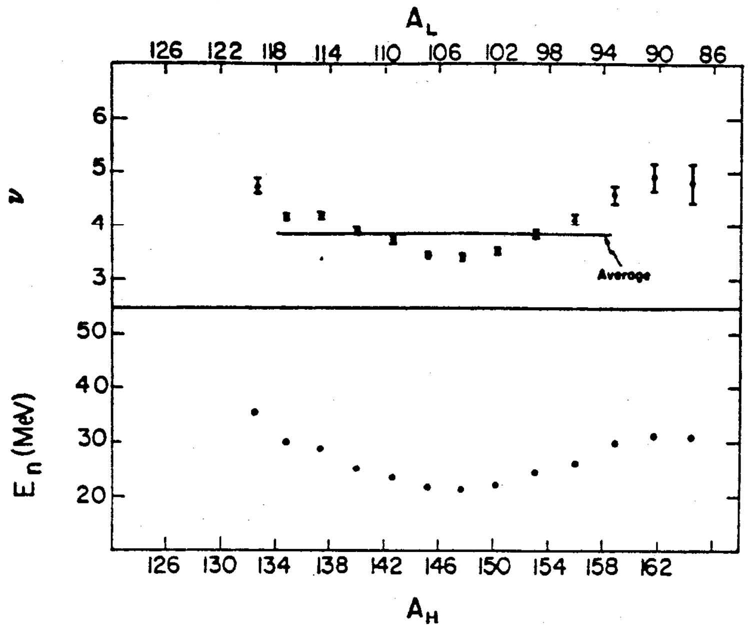

FIG. 8g-20. Total number of neutrons ν and total energy E_n appearing in the form of neutrons as a function of fragment mass. For reference, see Fig. 8g-17.

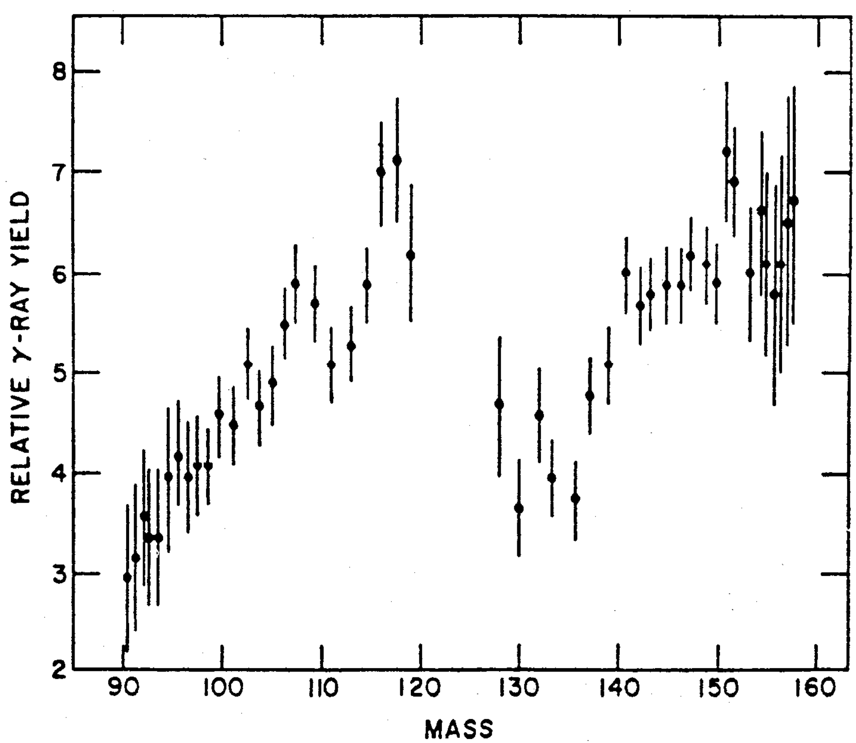

FIG. 8g-21. The γ-ray yield as a function of mass. [*S. A. E. Johansson, Nucl. Phys.* **60**, 378 (1964).]

TABLE 8g-10. CHARACTERISTICS OF PROMPT GAMMA RADIATIONS EMITTED IN FISSION*

Fissioning nuclide	Average no. of photons per fission	Average photon energy released per fission
$U^{235} + n_{th}$[a]	7.5	7.46
$U^{235} + n_{th}$[b]	7.2 ± 0.8	7.4 ± 0.8
$U^{235} + n_{th}$[c]	7.93 ± 0.48	9.51 ± 0.23
Cf^{252}[d]	10	9
Cf^{252}[e]	10.3	8.2

* From J. Gindler and J. R. Huizenga, Nuclear Fission, in "Nuclear Chemistry," vol. II., L. Yaffe, ed., Academic Press, Inc., New York, 1968.

[a] J. Francis and R. Gamble, *Oak Ridge Nat. Lab. Rept.* ORNL-1879 (unpublished).

[b] F. C. Maienschein, R. W. Peele, W. Zohel, and T. A. Love, *Proc. U.N. Intern. Conf. Peaceful Uses At. Energy (Geneva)* **15**, 366 (0.3 ≤ E_γ ≤ 10 MeV), (1958).

[c] F. E. W. Rau, *Ann. Physik* **10**, 252 (1963).

[d] H. R. Bowman and S. G. Thompson, *Proc. U.N. Intern. Conf. Peaceful Uses At. Energy (Geneva)* **15**, 212 (1958).

[e] A. Smith, P. Fields, A. Friedman, S. Cox, and R. Sjoblom, *ibid*, **15**, 392 (1958).

TABLE 8g-11. AVERAGE NUMBER AND ENERGY OF BETA DECAYS PER FISSION FOR U^{235} AND U^{233} THERMAL NEUTRON FISSION*

U^{235}		U^{233}
N_β	E_β	N_β
6.6 ± 0.9[a]		
6.9 ± 0.4[b]	8.1 ± 0.4[b]	
6.6 ± 0.2[c]		
5.93 ± 0.2[d]	....	5.25 ± 0.2[d]
6.10[f]	....	5.27[d]
	7.6 ± 0.5[e]	

* From J. Gindler and J. R. Huizenga, Nuclear Fission, in "Nuclear Chemistry," vol. II, L. Yaffe, ed., Academic Press, Inc., New York, 1968.

[a] G. Alzmann, *Nukleonik* **3**, 295 (1961).

[b] P. Armbruster and H. Meister, Z. Physik **170**, 274 (1962).

[c] P. Armbruster, D. Hovestadt, H. Meister, and H. J. Specht, *Nucl. Phys.* **54**, 586 (1964).

[d] H. J. Specht and H. Seyfarth, "Physics and Chemistry of Fission," vol. II, p. 253, IAEA, Vienna, 1965.

[e] J. F. Perkins and R. W. King, *Nucl. Sci. Eng.* **3**, 726 (1958).

[f] Calculated value.

TABLE 8g-12. CALIBRATION CONSTANTS FOR HEAVY-ION DETECTORS

Cf^{252}	U^{235}
$a = \dfrac{24.0203}{P_L - P_H}$	$a = \dfrac{30.9734}{P_L - P_H}$
$a' = \dfrac{0.03574}{P_L - P_H}$	$a' = \dfrac{0.04596}{P_L - P_H}$
$b = 89.6083 - aP_L$	$b = 87.8626 - aP_L$
$b' = 0.1370 - a'P_L$	$b' = 0.1345 - a'P_L$

TABLE 8g-13. LIMITS ON SPECTRUM SHAPE PARAMETERS

Spectrum characteristic	Cf^{252}	U^{235}
N_L N_V	>2.85	~ 19
N_H N_V	~ 2.2	~ 12.5
N_L N_V	1.30	1.49–1.55
ΔL $(L - H)$	$\lesssim 0.38$	0.22
ΔH $(L - H)$	$\lesssim 0.45$	0.35
$(H - HS)/(L - H)$	$\lesssim 0.70$	0.38
$(LS - L)/(L - H)$	$\lesssim 0.49$	0.27
$(LS - HS)/(L - H)$	$\lesssim 2.18$	~ 1.66

TABLE 8g-14. AVERAGE FRAGMENT ENERGIES AND MASSES FOR Cf^{252} SPONTANEOUS FISSION

$\langle V_H \rangle$	1.036 cm/nsec	$\langle E_L \rangle$	105.71 MeV
$\langle V_L \rangle$	1.375 cm/nsec	σ_{E_H}	8.43 MeV
$\sigma(V_H)$	0.0789 cm/nsec	σ_{E_L}	5.61 MeV
$\sigma(V_L)$	0.0650 cm/nsec	$\langle E_K \rangle$	185.7 MeV
$\langle M_H \rangle$	143.61 amu	σ_{E_K}	11.0 MeV
$\langle M_L \rangle$	108.39 amu	$\langle R_A \rangle$	1.334
$\sigma_{M_L} = \sigma_{M_H}$	6.72 amu	σ_{R_A}	0.137
$\langle E_H \rangle$	80.01 MeV		

All quantities are preneutron emission [S. L. Whetstone, *Phys. Rev.* **131**, 1232 (1963)].

TABLE 8g-15. CHARGED-PARTICLE YIELDS FROM Cf^{252} SPONTANEOUS FISSION

Particle	Yield, particles/fission	Particle	Yield, particles/fission
p	$(5.1 \pm 0.5)(10^{-5})$	He^6	$(7.8 \pm 1.6)(10^{-5})$
d	$(2.0 \pm 0.1)(10^{-5})$	He^8	$(5.9 \pm 1.6)(10^{-6})$
t	$(1.90 \pm 0.06)(10^{-4})$	He^{10}	$(3 \pm 3)(10^{-7})$
He^3	$\lesssim 2.9 \times 10^{-5}$	Li	$(3.9 \pm 2.0)(10^{-6})$
α	$(3.27 \pm 0.10)(10^{-3})$	Be	$>3 \times 10^{-7}$

From S. L. Whetstone and T. D. Thomas, *Phys. Rev.* **154**, 1174 (1967).

8g-5. Bibliography. For a comprehensive summary of nuclear fission data, the reader is referred to the following excellent sources:

1. Hyde, E. K.: "The Nuclear Properties of the Heavy Elements," vol. III, Prentice-Hall, Inc., Englewood Cliffs, N.J., 1964.
2. "Physics and Chemistry of Fission," vols. I and II, (IAEA, Vienna, 1965).
3. Gindler, J., and J. R. Huizenga: Nuclear Fission, in "Nuclear Chemistry," vol. II, L. Yaffe, ed., Academic, Press, Inc., New York, 1968.